JOC Article
pubs.acs.org/joc

Cofacial Boron Dipyrromethene (Bodipy) Dimers: Synthesis, Charge Delocalization, and Exciton Coupling

Andrew C. Benniston,*,† Graeme Copley,† Anthony Harriman,† David Howgego,† Ross W. Harrington,‡ and William Clegg‡

†Molecular Photonics Laboratory and ‡Crystallography Laboratory, Bedson Building, School of Chemistry, Newcastle University, Newcastle upon Tyne, NE1 7RU, United Kingdom

a.c.benniston@ncl.ac.uk

Received January 18, 2010

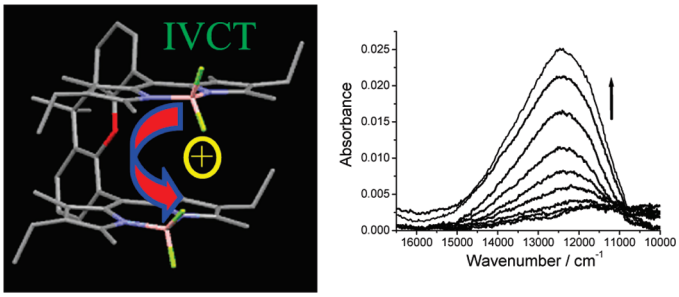

A series of compounds containing two boron dipyrromethene (Bodipy) units has been synthesized and fully characterized in which the spacer between the two Bodipy groups is varied from dibenzothiophene (**BD1**), to dibenzofuran (**BD2**), to 9,9-dimethylxanthene (**BD3**), and finally to diphenyl ether (**BD4** and **BD5**). For **BD1**−**BD4** the Bodipy units adopt, to varying degrees, cofacial conformations that allow for systematic variations of both the mutual orientation and the mean separation of the two Bodipy residues. In the remaining dimer, **BD5**, the Bodipy units are well-separated and cannot come into close proximity. Single-crystal X-ray structures have been determined for **BD1**−**BD3** and reveal that the "bite angle" between the two Bodipy residues decreases progressively along the series with individual values of 41.33(5)°, 36.95(6)°, and 8.57(3)°. Detailed ^{1}H and ^{19}F NMR studies for **BD3** and **BD4** show the methylene protons to be diastereotopic due to restricted rotation of the two Bodipy groups. For **BD4** conformational rocking is invoked to explain the variable-temperature NMR spectra, whereby the methyl and methylene groups become inequivalent. Cyclic voltammetry indicates reversible oxidation and reduction of the Bodipy groups. However, the close proximity of the Bodipy groups in **BD3** and **BD4** results in two well-resolved waves in the anodic region, and slight splitting of the cathodic wave. Peak splitting is attributed to charge delocalization. Spectroelectrochemical measurements at a fixed oxidative potential reveal an optical intervalence charge-transfer (IVCT) absorption band. This IVCT band is attributed to electron exchange between the cofacially arranged neutral and mono-oxidized Bodipy units. Various levels of exciton coupling are observed for **BD1**−**BD4**, but not **BD5** since here the Bodipy groups remain isolated.

Introduction

Strongly interacting pairs of chromophores held in cofacial, π-stacked arrangements are found in several biological environments, such as the base pairs within duplex DNA,[1,2] the primary electron donor in bacterial photosynthetic reaction center proteins,[3] and pigments in light-harvesting complexes.[4] Artificial analogues have found many applications in both catalysis and molecular photonics. In extreme cases,

(1) Watson, J, D.; Crick, H. H. C. *Nature* **1953**, *171*, 737.
(2) (a) Yakovchuck, P.; Protozanova, E.; Frank-Kamenetskii, M. D. *Nucleic Acids Res.* **2006**, *34*, 564. (b) Kool, E. T. *Ann. Rev. Biophys. Struct.* **2001**, *30*, 1. (c) Waters, M. L. *Curr. Opin. Chem. Biol.* **2002**, *6*, 736.
(3) Shipman, L. L.; Cotton, T. M.; Norris, J. R.; Katz, J. J. *Proc. Natl. Acad. Sci. U.S.A.* **1976**, *73*, 1791.
(4) (a) Deisenhofer, J.; Epp, O.; Miki, R.; Huber, R.; Michel, H. *J. Mol. Biol.* **1984**, *180*, 385. (b) Deisenhofer, J.; Epp, O.; Miki, R.; Huber, R.; Michel, H. *Nature* **1985**, *318*, 618.

Published on Web 02/15/2010 DOI: 10.1021/jo1000803

individual molecules are held tightly in a cofacial manner that leads to pronounced exciton coupling.[5] Such high levels of π-electron interaction cause a splitting of respective absorption transitions localized on the chromophores and can result in the creation of low-energy absorbing species. In turn, this situation can provide a favorable driving force for the trapping of harvested photons or a molecular sequence possessing a perturbed reduction potential.[6] Both cases, by virtue of installing low-energy sinks into a network of identical molecular entities, have the effect of introducing selectivity at a particular site created by loose association of chromophores or redox-active reagents. There has been much interest in designing artificial analogues, often using metalloporphyrins as the building blocks, under conditions where detailed spectroscopic investigations can be carried out.[7] More limited attention has been paid to π-stacking of boron dipyrromethene (Bodipy) dyes, these molecules being extremely fluorescent in solution, as a simple means of probing biological environments.[8−17] Indeed, it has been established that when biomolecules are labeled with Bodipy residues at relatively high dye/protein ratios it is plausible for two Bodipy residues to come into close proximity, thereby resulting in quenching of the fluorescence and/or formation of a bathochromically shifted excimer band.[18] Such self-association can be used to probe distances between specific regions in proteins, and also to monitor lipid packing effects within living cells. In these systems, however, the Bodipy linkages are highly flexible and give rise to a multitude of possible geometries, some of which are emissive while others remain nonfluorescent. This situation hinders establishment of a generic relationship between the geometry and the level of exciton coupling. No attention has been given to the redox properties of such Bodipy-based dimers.

Considering the relative ease of synthetic manipulation of Bodipy dyes,[19] it is clear that strategically positioned dimers may well become the next subclass of this ever-growing family of organic dyes. Consequently, we have developed an approach for the assembly of Bodipy units into rigid, cofacial arrangements whereby the spacer unit is changed systematically so as to control both the mutual orientation and internucleus separation distance.[20] The basic strategy follows that established earlier for the construction of cofacial porphyrin-based dimers.[21] The series starts with dibenzothiophene as a spacer unit. Here, the large radius of the sulfur atom provides an extended "bite angle" between adjacent Bodipy chromophores (the dihedral angle between mean planes), resulting in restricted interactions between the two units. The second spacer is dibenzofuran, which serves to decrease the "bite angle" and bring the Bodipy residues into closer proximity. A more extreme case is realized with 9,9-dimethylxanthene as the spacer unit.[20] Here the Bodipy units are locked rigidly in a coplanar fashion that leads to severe exciton interactions between the adjacent Bodipy units. Finally, to complement this series, an additional dimer has been synthesized around a flexible spacer that provides the Bodipy units with a high degree of conformational freedom. A benefit of using Bodipy dyes is that, compared to porphyrin[21] and perylenediimide residues,[22] only a single transition dipole vector has to be considered. Nonetheless, the success of any detailed spectroscopic study rests on the availability of structural information for the dimers both in the solid state and in solution. The present investigation covers the synthesis, characterization, and preliminary spectroscopic examination of the series of cofacial dyes. Later work will focus on establishing a comprehensive understanding of the exciton interactions in solution.

Results and Discussion

Synthesis. The synthetic strategy (Scheme 1) employed to isolate the Bodipy-based dimers is a linear approach that

(5) Kasha, M.; Rawls, H, R.; El-Bayoumi. *Pure Appl. Chem.* **1965**, *11*, 371.

(6) (a) Wasielewski, M. R. *Chem. Rev.* **1992**, *92*, 435. (b) Kobuke, Y. *Eur. J. Org. Chem.* **2006**, 2333. (c) van Grondelle, R.; Dekker, J. P.; Gillbro, T.; Sundstrom, V. *Biochim. Biophys. Acta* **1994**, *1187*, 1. (d) Ozeki, H.; Nomoto, A.; Ogawa, K.; Kobuke, Y.; Murakami, M.; Hosoda, K.; Ohtani, M.; Nakashima, S.; Miyasaka, H.; Okada, T. *Chem.—Eur. J.* **2004**, *10*, 6393.

(7) (a) Palacios, R. E.; Gould, S. L.; Herrero, C.; Hambourger, M.; Brune, A.; Kodis, G.; Liddell, P. A.; Kennis, J.; Macpherson, A. N.; Gust, D.; Moore, T. A.; Moore, A. L. *Pure Appl. Chem.* **2005**, *77*, 1001. (b) Collin, J.-P.; Harriman, A.; Heitz, V.; Odobel, F.; Sauvage, J.-P. *J. Am. Chem. Soc.* **1994**, *116*, 5679. (c) Rodriquez, J.; Kirmaier, C.; Johnson, M. R.; Friesner, R. A.; Holten, D.; Sessler, J. L. *J. Am. Chem. Soc.* **1991**, *113*, 1652. (d) Wynne, K.; LeCours, S. M.; Galli, C.; Therien, M. J.; Hochstrasser, R. M. *J. Am. Chem. Soc.* **1995**, *117*, 3749. (e) Heitele, H.; Pöllinger, F.; Häberle, T.; Michel-Beyerle, M. E.; Staab, H. A. *J. Phys. Chem.* **1994**, *98*, 7402. (f) Palacios, R. E.; Kodis, G.; Gould, S. L.; de la Garza, L.; Brune, A.; Gust, D.; Moore, T. A.; Moore, A. L. *ChemPhysChem* **2005**, *6*, 2359. (g) Hayes, R. T.; Wasielewski, M. R.; Gosztola, D. *J. Am. Chem. Soc.* **2000**, *122*, 5563. (h) Benniston, A. C.; Harriman, A.; Li, P. *J. Am. Chem. Soc.* **2010**, *132*, 26.

(8) Ji, D.; Zhao, R.; Huang, Z.; Xia, A. *J. Lumin.* **2007**, *122*, 253.

(9) Shi, X.; Duft, D.; Parks, J. H. *J. Phys. Chem. B* **2008**, *112*, 12801.

(10) Karolin, J.; Fa, M.; Wilczynska, M.; Ny, T.; Johansson, L. B. A. *Biophys. J.* **1998**, *74*, 11.

(11) Fa, M.; Bergström, F.; Hägglöf, P.; Wilczynska, M.; Johansson, L. B. A. *Structure* **2000**, *8*, 397.

(12) Tleugabulova, D.; Zhang, Z.; Brennan, J. D. *J. Phys. Chem. B* **2002**, *106*, 13133.

(13) Jones, L. J.; Upson, R. H.; Haugland, R. P.; Panchuck-Voloshina, N.; Zhou, M. *Anal. Biochem.* **1997**, *251*, 144.

(14) Jiang, P.; Mellors, A. *Anal. Biochem.* **1998**, *259*, 8.

(15) Da Poian, A. T.; Gomes, A. M. O.; Coelho-Sampaio, T. *J. Virol. Meth.* **1998**, *70*, 45.

(16) Thompson, V. F.; Saldana, S.; Cong, J.; Goll, D. E. *Anal. Biochem.* **2000**, *279*, 170.

(17) Welder, F.; Moody, E.; Colyer, C. L. *Electrophoresis* **2002**, *23*, 1585.

(18) Bergström, F.; Mikhalyov, I.; Hägglöf, P.; Wortmann, R.; Ny, T.; Johansson, L. B. A. *J. Am. Chem. Soc.* **2002**, *124*, 196.

(19) (a) Loudet, A.; Burgess, K. *Chem. Rev.* **2007**, *107*, 4891. (b) Wood, T. E.; Thompson, A. *Chem. Rev.* **2007**, *107*, 1831.

(20) A xanthene-based Bodipy dimer has been prepared previously but no systematic alteration in the spacer was attempted, see: Saki, N.; Dinc, T.; Akkaya, E, U. *Tetrahedron* **2006**, *62*, 2721. For an example where the unit has been used previously in porphyrin systems see: Deng, Y.; Chang, C. J.; Nocera, D. G. *J. Am. Chem. Soc.* **2000**, *122*, 410.

(21) (a) Gong, Y.; Xie, J.; Xia, A.; Shao, X.; Li, Z. *J. Lumin.* **2007**, *122*, 250. (b) Nobukuni, H.; Shimazaki, Y.; Tani, F.; Naruta, Y. *Angew. Chem., Int. Ed.* **2007**, *46*, 8975. (c) Fillers, J. P.; Ravichandran, K. G.; Abdalmuhdi, I.; Tulinsky, A.; Chang, C. K. *J. Am. Chem. Soc.* **1986**, *108*, 417. (d) Bolze, F.; Gros, C. P.; Drouin, M.; Espinosa, E.; Harvey, P. D.; Guilard, R. *J. Organomet. Chem.* **2002**, *643*, 89. (e) Faure, S.; Stern, C.; Guilard, R.; Harvey, P. D. *J. Am. Chem. Soc.* **2004**, *126*, 1253. (f) Osuka, A.; Maruyama, K. *J. Am. Chem. Soc.* **1988**, *110*, 4454. (g) Leighton, P.; Cowan, J. A.; Abraham, R. J.; Sanders, J. K. M. *J. Org. Chem.* **1988**, *53*, 733. (h) Fletcher, J. T.; Therien, M. J. *J. Am. Chem. Soc.* **2002**, *124*, 4298. (i) Satake, A.; Kobuke, Y. *Org. Biomol. Chem.* **2007**, *5*, 1679.

(22) (a) Giaimo, J. M.; Gusev, A. V.; Wasielewski, M. R. *J. Am. Chem. Soc.* **2002**, *124*, 8530. (b) Hariharan, M.; Zheng, Y.; Long, H.; Zeidan, T. A.; Schatz, G. C.; Vura-Wies, J.; Wasielewski, M. R.; Zuo, X.; Tiede, D. M.; Lewis, F. D. *J. Am. Chem. Soc.* **2009**, *131*, 5920. (c) Bhosale, S.; Sisson, A. L.; Talukdar, P.; Fürstenberg, A.; Banerji, N.; Vauthey, E.; Bollot, G.; Mareda, J.; Röger, C.; Würthner, F.; Sakai, N.; Matile, S. *Science* **2006**, *313*, 84. (d) Samori, P.; Fechtenkötter, A.; Reuther, E.; Watson, M. D.; Severin, N.; Müllen, K.; Rabe, J. P. *Adv. Mater.* **2006**, *18*, 1317. (e) Xu, W.; Chen, H.; Wang, Y.; Zhao, C.; Li, X.; Wang, S.; Weng, Z. *ChemPhysChem* **2008**, *9*, 1409. (f) Tang, T.; Herrmann, A.; Peneva, K.; Müllen, K.; Webber, S. E. *Langmuir* **2007**, *23*, 4623.

SCHEME 1[a]

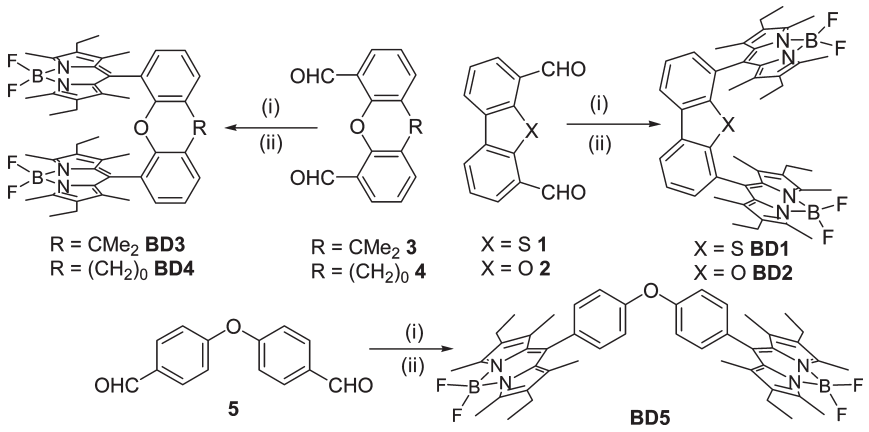

[a]Reagents and conditions: (i) 3-ethyl-2,4-dimethyl-1*H*-pyrrole, DCM, TFA, rt. (ii) DDQ; *N*,*N*-diisopropylethylamine, $BF_3 \cdot Et_2O$.

involves building directly from the bare spacer unit, a tactic that has been utilized previously for constructing cofacial metalloporphyrin dimers.[23] The target dialdehydes were prepared by literature procedures[24−28] and subjected to standard Bodipy-forming conditions,[29] doubling the equivalents of required reactants. The yields for the formation of the Bodipy dimers were 23% for the dibenzothiophene scaffold (**BD1**), 18% for dibenzofuran (**BD2**), but only 5% for 9,9-dimethylxanthene (**BD3**). The poor yield for this last compound can be rationalized on the basis of the crystal structure discussed shortly; namely, steric hindrance is encountered between fluorine atoms on adjacent Bodipy residues, thereby creating a staggered conformation in the crystal. A further compound, **BD4**, incorporating a flexible spacer, was synthesized in 16% yield. It was anticipated that this fourth compound would have the ability to adopt both open and closed conformations as is indicated by molecular modeling studies. The final control compound, **BD5**, was produced in 26% yield, and represents a dyad where intramolecular interactions between the Bodipy centers are improbable. All compounds were characterized fully by conventional analytical techniques, including NMR spectroscopy (^{1}H, ^{13}C, ^{19}F, ^{11}B), mass spectrometry, elemental analysis, and melting points. These materials were soluble to various degrees in common organic solvents.

Structure Determination. A critical feature for this research program relates to establishing ground-state geometries for each of the constrained dimers. For this reason, suitable crystals were grown by slow evaporation techniques. After exploring several solvent mixtures, X-ray diffraction quality single crystals were obtained for **BD1**, **BD2**, and **BD3**, although crystals of two of these were small and weakly diffracting, requiring synchrotron radiation for successful investigation. The molecular structures for these three compounds are shown in Figure 1. Although we are aware of the potential impact of crystal packing forces and of thermal motions in solution, we can use the X-ray data as the starting point for analysis of the spectroscopic data. As such, an important point concerns the so-called "bite angle" for the dimer; this is the dihedral angle subtended between the two Bodipy mean planes. The values derived for **BD1**, **BD2**, and **BD3** are 41.33(5)°, 36.95(6)°, and 8.57(3)°, respectively. This trend follows that expected on the basis of the stereochemistry of the bridge. It is notable that **BD3**, for which the molecule has an exact crystallographic C_2 axis through the O and CMe_2 groups of the bridge, experiences significant internal strain due to close positioning of the fluorine atoms and this causes adoption of a staggered geometry (Figure 1C). As the fluorine atoms attempt to avoid each other, both the Bodipy residues deviate out of perpendicular alignment with the 9,9-dimethylxanthene scaffold by 13.60(2)°, in comparison to only 2.86(3)° and 0.59(3)° in the case of **BD1** and 1.00(4)° and 3.35(4)° for **BD2** (neither of these molecules has crystallographic symmetry, though both are close to C_{2v} ignoring differences in ethyl group orientations).

This staggered conformation leads to some interesting ^{1}H and ^{19}F NMR findings to be discussed in the next section. ^{19}F NMR can be used to suggest that rotation of the Bodipy residues occurs freely in the case of **BD1** but not for either **BD2** or **BD3**. The radius of the Bodipy residue in these compounds, or the radius of the rotor, is 4.86 Å (measured from the CH_2 of the ethyl group to the center point of the indacene core). In the case of **BD1**, the distance between the *meso* positions on adjacent Bodipy units was calculated to be 6.35 Å, and the distance between adjacent boron atoms was measured to be 8.52 Å; the corresponding distances for **BD3** are 4.56 and 5.05 Å, respectively. Applying the space-filling model (see the Supporting Information) to take account of interactions between van der Waals radii, it seems reasonable

(23) (a) Yagi, S.; Yonekura, I.; Awakura, M.; Ezoe, M.; Takagishi, T. *Chem. Commun.* **2001**, 557. (b) Morisue, M.; Haruta, N.; Kalita, D.; Kobuke, Y. *Chem.—Eur. J.* **2006**, *12*, 8123. (c) Faure, S.; Stern, C.; Espinosa, R.; Douville, J.; Guilard, R.; Harvey, P. *Chem.—Eur. J.* **2005**, *11*, 3469. (d) Hiom, J.; Paine, J. B. III; Zapf, U.; Dolphin, D. *Can. J. Chem.* **1983**, *61*, 2220. (e) Collman, J. P.; Bencosme, C. S.; Durand, R. R. Jr; Kreh, R. P.; Anson, F. C. *J. Am. Chem. Soc.* **1983**, *105*, 2699.

(24) Skar, M. L.; Svendsen, J. S. *Tetrahedron* **1997**, *53*, 17425.

(25) Kuehm-Caubère, C.; Adach-Becker, S.; Fort, Y.; Caubère, P. *Tetrahedron* **1996**, *52*, 9087.

(26) Nagamani, S. A.; Norikane, Y.; Tamaoki, N. *J. Org. Chem.* **2005**, *70*, 9304.

(27) Osuka, A.; Kobayashi, F.; Maruyama, K. *Bull. Chem. Soc. Jpn.* **1991**, *64*, 1213.

(28) Kuhnert, N.; Burzlaff, N.; Patel, C.; Lopez-Periago, A. *Org. Biomol. Chem.* **2005**, *3*, 1911.

(29) (a) Wu, L.; Burgess, K. *Chem. Commun.* **2008**, 4933. (b) Shah, K.; Thangraj, K.; Soong, M. L.; Wolford, L.; Boyer, J. H.; Politzer, I. R.; Pavlopoulos, T. G. *Heteroat. Chem* **1990**, *1*, 389. (c) Burghart, A.; Kim, H.; Welch, M. B.; Thorensen, L. H.; Reibenspies, J.; Burgess, K. *J. Org. Chem.* **1999**, *64*, 7813.

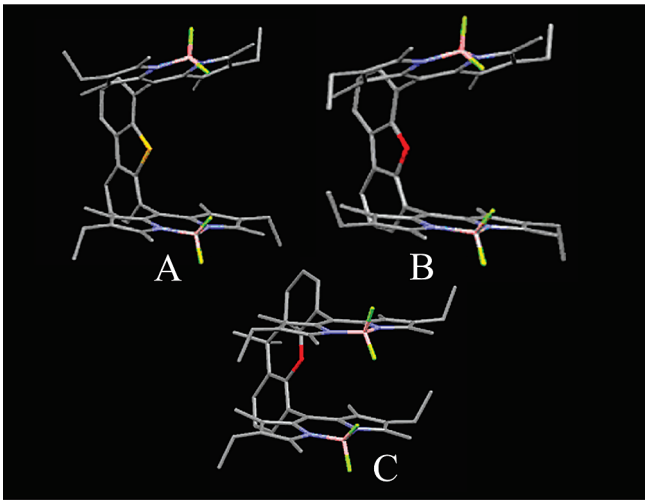

FIGURE 1. X-ray molecular structures for **BD1** (A), **BD2** (B), and **BD3** (C): carbon (gray), oxygen (red), nitrogen (blue), boron (purple), fluorine (green). The hydrogen atoms have been removed for clarity as well as any solvent molecules.

to suggest that the Bodipy units within **BD1** can rotate in a cooperative fashion. In the case of **BD2**, where ^{19}F NMR indicates the beginning of restricted rotation of the Bodipy units, the distance between the *meso* positions on adjacent Bodipy units was measured as 5.65 Å, while the distance between adjacent boron atoms was 7.56 Å. These values are considerably smaller than that for **BD1**. Again applying the space-filling model to the molecular structure of **BD2** (see the Supporting Information) emphasizes the significantly smaller volume available for internal rotation of the Bodipy units, and draws attention to the clashing methyl groups appended at the 1- and 7-positions of adjacent Bodipy residues.

^{1}H NMR Spectroscopy. The X-ray data, while confirming authenticity of the compounds and providing a starting point for discussion of the molecular structures, cannot be relied upon for precise conformational information in solution. For this purpose, detailed NMR studies were undertaken. Now, close inspection of the ^{1}H NMR spectra for the constrained dimers indicates that the scaffold plays an important role in controlling the various coupling patterns, some of which are unexpectedly complex. Thus, for **BD5** the ethyl groups appended to the Bodipy cores appear as a triplet and a quartet in the ^{1}H NMR spectrum (see the Supporting Information). It should be noted that each methylene group for the two Bodipy centers is prochiral and several stereoisomers are to be anticipated (see the Supporting Information). That no complex coupling patterns are seen for **BD5** (and also for simple Bodipy derivatives) implies that each methylene group remains homotopic/enantiotopic and the protons are not coupled.[30] In comparison, the signals for the CH_2 groups displayed in the ^{1}H NMR spectra of **BD3** and **BD4** show a much greater degree of complexity. For example, for **BD3** the corresponding signals for the CH_2 groups (Figure 2) comprise a total of 12 lines. This complex splitting pattern is a clear indication that the two hydrogen

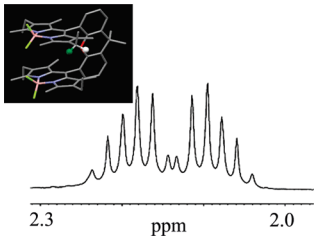

FIGURE 2. Partial ^{1}H NMR spectrum for **BD3** collected from d_8-THF solution at room temperature, showing the proton resonances for the methylene group of the four ethyl units. The inset shows the two diastereotopic protons (green and white) for one of the methylene groups.

SCHEME 2. Basic Representation of the Rocking-like Conformational Exchange Proposed for BD4

atoms differ, and in fact they are more analogous to diastereotopic protons that couple both to each other and to the methyl protons.[31] For **BD3** the observed coupling patterns are linked to some structural facet, the most straightforward being a locked geometry that severely restricts rotation of the two Bodipy units. Such constraint means that the two faces of each dipyrrin are environmentally different in a manner reminiscent of the introduction of a plane of chirality.[32] Thus, the hydrogen atoms of the CH_2 group are inequivalent due to the different environments in which they reside. A simple inspection of the crystal structure of **BD3** highlights this point, as shown in the insert to Figure 2, where the diastereotopic hydrogens are marked green and white. First, each magnetically distinct CH_2 proton is split into a doublet, and the adjacent terminal CH_3 group of the corresponding ethyl group then splits both doublets into quartets. The overall signal should consist of two doublets of quartets (16 lines). In Figure 2 only 12 of these 16 lines can be resolved, because of overlapping signals of comparable chemical shift. The effect of diastereotopic protons is also observed in the ^{1}H NMR spectrum of **BD4** (see the Supporting Information), although the effect is less pronounced than for **BD3** owing to the disparity in conformational rigidity. In the case of **BD4**, only 9 of the expected 16 lines are resolved at 400 MHz.

For **BD2**, where restricted rotation of the Bodipy units is somewhat relaxed, the relevant CH_2 splitting pattern appears as a quartet due to the summation of overlapping peaks, with much smaller peaks appearing on the side of the main peak. These satellite peaks become more apparent at lower temperature (see the Supporting Information), and are not a product of spinning side bands, since these are absent from all other peaks. The combined information from these ^{1}H NMR experiments is supportive of the notion that the prochirality is a product of restricted rotation. Indeed, the ^{1}H NMR spectrum of **BD1** exhibits a standard quartet.

(30) Because of the Bodipy dipyrrin plane the two fluorines are equivalent for all stereoisomers due to the two methylene prochiral centers (see the Supporting Information). This criterion is removed once the two faces become inequivalent when free rotation around the meso bond is no longer possible. The BF_2 unit can be viewed as a prochiral center in the dimers.

(31) Silverstein, R. M.; Webster, F. X. *Spectroscopic Identification of Organic Compounds*, 6th ed.; John Wiley & Sons, Inc.: New York, 1998.

(32) IUPAC. *Compendium of Chemical Terminology*, 2nd ed. (the "Gold Book"); compiled by McNaught, A. D., Wilkinson, A.; Blackwell Scientific Publications: Oxford, UK, 1997.

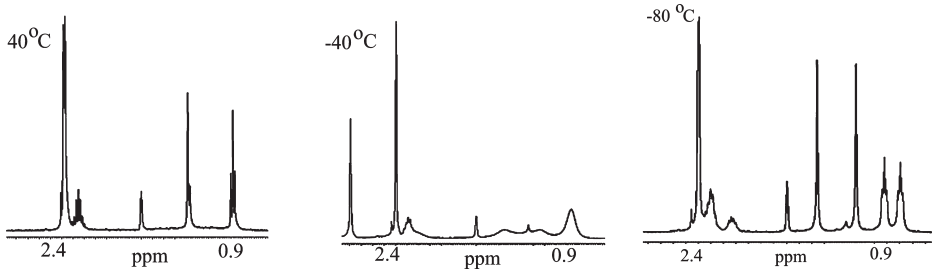

FIGURE 3. Partial ^{1}H NMR spectra recorded for **BD4** at various temperatures in d_8-THF.

Temperature-dependent ^{1}H NMR studies have highlighted that **BD4** exists in a staggered conformation, similar to **BD3**, but with the compound rapidly exchanging between the two extreme forms of the staggered conformation via a rocking-like process (Scheme 2). Similar studies performed with **BD1**, **BD2**, **BD3**, and **BD5** in d_8-THF over a temperature range from −80 to 60 °C showed the spectrum to be insensitive to temperature, except for a small alteration of the CH_2 quartet profile with respect to **BD4**. However, some subtle changes were observed in the corresponding ^{1}H NMR spectrum of **BD4** in d_8-THF over the same temperature range (Figure 3).

As can be seen from inspection of Figure 3, the ^{1}H NMR spectrum recorded for **BD4** at 40 °C displays the expected triplet for the CH_3 group of the ethyl group, two methyl resonances corresponding to the two different indacene core methyl group environments within a symmetrical Bodipy compound, and the prochiral splitting pattern of the CH_2 group related to restricted rotation of the Bodipy units. As the temperature is lowered to −40 °C, the triplet broadens and begins to split into two signals, corresponding to inequivalence of the ethyl groups for the two Bodipy units. Furthermore, the CH_2 groups also become inequivalent on each Bodipy unit since the original prochiral splitting pattern for the CH_2 group starts to separate into two distinct signals. Finally, at −80 °C all the methyl groups become inequivalent within each Bodipy unit, suggesting asymmetry has been introduced. These observations are in line with the model highlighted in Scheme 2.

^{19}F NMR Spectroscopy. ^{19}F NMR spectroscopy is an extremely useful tool that provides definitive information for the rotational freedom of Bodipy units, or indeed functional groups within Bodipy compounds.[33] In the case of the dimers under investigation here, ^{19}F NMR spectroscopy can be used to probe rotational freedom of the individual Bodipy residues. Starting with **BD1**, this derivative possessing the largest "bite angle", the ^{19}F NMR spectrum indicates complete rotational freedom of the Bodipy units on the NMR time scale, since a standard quartet is observed similar to those reported previously for simple Bodipy compounds (see the Supporting Information). The ^{19}F NMR spectrum recorded for **BD2**, however, displays inequivalence of the fluorine atoms due to the smaller "bite angle" in comparison to **BD1**, resulting in restricted rotation of the Bodipy units on the NMR time scale (see the Supporting Information).

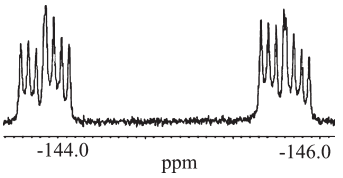

FIGURE 4. The ^{19}F NMR spectrum of **BD3** recorded in d_8-THF at room temperature.

Considering the crystal structure of **BD2** (Figure 1), it is clear that restricted rotation creates disparate environments around the fluorine atoms, with two fluorine atoms pointing toward the center and the remaining pair being directed away from the center.

Again, variable-temperature studies were performed in an effort to measure the rotational barriers for the dimers. However, ^{19}F NMR studies carried out for each compound in d_8-THF over a temperature range of −80 to 60 °C showed no change in the spectrum. Inequivalence of the fluorine atoms is again seen for **BD3**, but the effect is more pronounced due to the strained and compact nature of this compound (Figure 4). Here, the chemical shift difference between the fluorine resonances is 2.65 ppm, in comparison to 1.25 ppm for **BD2**. Similar results were observed with **BD4** but the control compound **BD5** gave a standard quartet that remained unaffected by changes in temperature.

Electrochemical Investigations. A preliminary examination of the electrochemical behavior of the various Bodipy dimers was carried out in CH_2Cl_2 (0.2 M TBATFB) by cyclic voltammetry under comparable conditions. The cyclic voltammogram recorded for the control compound **BD5** can be interpreted in terms of the known electrochemical behavior of mononuclear Bodipy derivatives.[34] Thus, each of the Bodipy units undergoes one-electron oxidation and reduction steps to form the respective radical ions. There is no indication for electronic or electrostatic interaction between the two units. The half-wave potentials derived for each of the electrochemical steps, which are quasireversible, are collected in Table 1. There is no sign of electrochemical activity associated with the spacer group.

The cyclic voltammograms recorded for **BD1** and **BD2** are similar. On reductive scans, a reversible, two-electron wave is seen that most likely corresponds to the simultaneous addition of one electron to each Bodipy unit. The half-wave potential is ca. 80 mV more negative than that found for the control compound (Table 1) but it is not obvious that the two

(33) (a) Benniston, A. C.; Copley, G.; Elliott, K. J.; Harrington, R. W.; Clegg, W. *Eur. J. Org. Chem.* **2008**, 2705. (b) Bröring, M.; Krüger, R.; Link, S.; Kleeberg, C.; Köhler, S.; Xie, X.; Ventura, B.; Flamigni, L. *Chem.—Eur. J.* **2008**, *14*, 2976. (c) Benniston, A. C.; Harriman, A.; Whittle, V. L.; Zelzer, M. *Eur. J. Org. Chem.* **2010**, 523.

(34) (a) Zhou, Y.; Xiao, Y.; Li, D.; Fu, M.; Qian, X. *J. Org. Chem.* **2008**, *73*, 1571. (b) Chen, J.; Burghart, A.; Derecskei-Kovacs, A.; Burgess, K. *J. Org. Chem.* **2000**, *65*, 2900.

TABLE 1. Electrochemical Potentials Recorded for the Dimers vs Fc^+/Fc

compd	E_1^a/V	E_2^b/V	E_3^c/V	E_4^d/V	ΔE^e/V
BD1		−1.67	0.57	0.64	2.24
BD2		−1.65	0.59	0.69	2.24
BD3	−2.08	−1.91	0.51	0.77	2.42
BD4	−1.96	−1.81	0.53	0.74	2.34
BD5		−1.75	0.64		2.39

[a] $E_1 = E_{1/2}$ for the one-electron reduction of the second Bodipy unit. [b] $E_2 = E_{1/2}$ for the one-electron reduction of the first Bodipy. [c] $E_3 = E_{1/2}$ for the one-electron oxidation of the Bodipy. [d] $E_4 = E_{1/2}$ for the one-electron oxidation of the second Bodipy. [e] $\Delta E = E_3 - E_2$.

radical ions communicate in an electronic sense. However, the peak separation (ΔE_P = 100 mV) is markedly smaller than that found for the control compound (ΔE_P = 250 mV) under identical conditions. On oxidative scans, the peak is split by ca. 100 mV for **BD2** and by ca. 70 mV for **BD1**, showing that the two Bodipy units are in electronic communication in these compounds. The splitting is modest but definite, unlike the situation seen on reductive scans, and is observed on both forward and reverse directions. The most likely explanation is that removal of an electron from the first Bodipy unit introduces an electrostatic barrier to removal of the electron from the second unit. Alternatively, the initial oxidizing equivalent could be delocalized over both Bodipy units. The net effect would be the same. The former case, however, raises the question as to why a comparable effect is not seen at the reductive stage? Perhaps there is a subtle structural change accompanying the electrochemical event that brings the rings closer together on oxidation but pushes them further apart on reduction. We will return to this point after scrutiny of the cyclic voltammograms collected for the other compounds. It is notable, however, that oxidation is somewhat easier for these dimers than for the control compound, while reduction is slightly more difficult.

Moving to the cyclic voltammetry carried out with **BD3**, both reductive and oxidative peaks are split into two one-electron steps. In fact, the reductive process is now well-resolved with the peaks being split by ca. 170 mV, while remaining quasireversible (see the Supporting Information). The oxidative wave is likewise split, but here the splitting is increased to 260 mV. Relative to the control, oxidation is much easier but reduction is more difficult. For the remaining dimer, **BD4**, both oxidative (ΔE = 210 mV) and reductive (ΔE = 150 mV) waves are split (Figure 5) while remaining quasireversible. The half-wave potentials for addition or removal of the first electron are less extreme than those found for **BD3**.

Using the values collected in Table 1, we can attempt to rationalize the electrochemical behavior in terms of the molecular topology. The control compound, which does not allow close contact between two Bodipy units, possesses two isolated units, and there is no detectable electronic interaction between these head groups. The behaviors of **BD1** and **BD2** are comparable and while the Bodipy head groups are in close contact they do not adopt cofacial geometries in the ground state. Oxidation is easier than for the control while reduction is slightly harder. Moreover, the oxidative peak is split by some 80 mV. Subtle differences exist between the two compounds, with the split in the oxidative peak for **BD1** being slightly smaller than that for **BD2**. All available evidence suggests that a cofacial arrangement is more likely for **BD2** than for **BD1**, although the

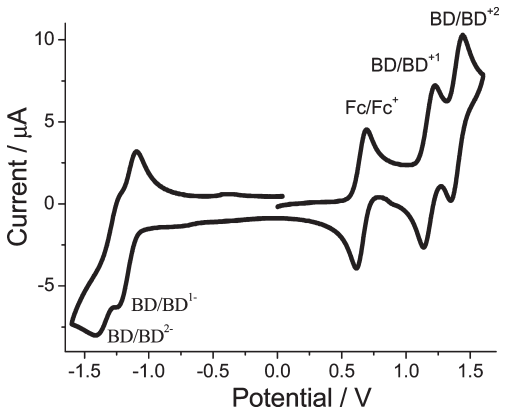

FIGURE 5. The cyclic voltammogram recorded for **BD4** in N_2-purged dry CH_2Cl_2 (0.2 M TBATFB). Scan rate = 100 mV s^{-1}.

molecular topology is far from ideal for this purpose. Having adopted the cofacial structure, electronic charge can be readily delocalized over the two head groups. The cyclic voltammetry results can be used to infer that only the oxidized species evolves into the cofacial geometry, with the reduced form minimizing orbital overlap between the Bodipy units.

For **BD3** both oxidative and reductive steps are resolved into successive one-electron events. The peak splitting is more pronounced for oxidation than for reduction, in line with the behavior reported above. Now, addition of the first electron is more difficult than that for any of the other compounds while removal of the first electron is much easier than that for other members of the series. This electronic effect is most likely related to the move to a spacer group that holds the Bodipy units in a cofacial arrangement and raises electron density over the entity. The peak splitting is attributed to delocalization of the electronic charge over the two Bodipy units. Similar delocalization effects are apparent for **BD4**, although the inherent flexibility of this molecule does not favor adoption of a cofacial arrangement for the ground state. This has the effect of making addition or removal of an electron similar to that of the control compound. This observation is in line with previous reports by Barbe and co-workers[35] concerning a series of cofacial porphyrin dimers. They concluded that the ease of removing an electron from the first porphyrin in comparison to a single porphyrin unit is due to the stabilization of the radical cation by $\pi-\pi$ interactions of closely spaced porphyrin rings.

Our understanding of the electrochemistry of these dimers assigns a key role to the mutual affects of closely aligned π-electron clouds. This effect is especially important for **BD3** where the topology forces the two Bodipy units to adopt a cofacial arrangement. The overlapping π-clouds render the molecule easier to oxidize but more difficult to reduce. The resulting delocalization of the charge over the two Bodipy units causes splitting of the peaks in the cyclic voltammogram. Perturbing the dihedral angle aligning the Bodipy units has a pronounced effect on the extent to which the π-clouds interact. Under oxidative conditions, removal of one electron can be stabilized by interaction with the second π-cloud but this effect is less significant for reductive

(35) Takai, A.; Gros, C, P.; Barbe, J.-M.; Guilard, R.; Fukuzumi, S. *Chem.—Eur. J.* **2009**, *15*, 3110.

processes. An interesting case concerns **BD4**, which has sufficient internal flexibility to reside in both closed and open conformations. The ease of addition or removal of an electron suggests that the ground-state geometry has the Bodipy units existing in a more open conformation. However, on reduction or oxidation the two head groups move into closer proximity so as to facilitate electron delocalization, as is evident from the peak splitting. On this basis, it can be concluded that charge delocalization is able to compensate for the electrostatic repulsion inherent to the reductive process.

Spectroelectrochemical Investigations. Further information on the effects of charge delocalization was sought from a series of spectroelectrochemical experiments carried out with use of a standard OTTLE cell and controlled-potential electrolysis. First, the dimers were subjected to oxidative conditions with a fixed potential at +1.0 V vs Fc^+/Fc, and recording absorption spectra at intervals of 1 min. For the control compound, these studies were consistent with formation of the stable cation radical. Again, the behavior of **BD1** and **BD2** was comparable and only the spectral data for the latter are shown (Figure 6). It will be noted that the spectra recorded before electrolysis show varying degrees of exciton coupling but discussion of this point will be delayed until the next section.

The absorbance due to **BD2** is diminished as electrolysis proceeds, while the exciton splitting of the main absorption transition becomes lost as oxidation proceeds. This bleaching of the main absorption band is accompanied by the growth of two new bands, one being on the high-energy shoulder of the S_0-S_1 electronic transition associated with the Bodipy unit and the other appearing at much lower energy. The absorption band centered at ca. 17 200 cm^{-1} can be attributed to the Bodipy π-radical cation,[36] this being consistent with reports in the literature and with our results on various monomeric compounds. The lowest energy absorption band is assigned to an intervalence charge-transfer (IVCT) transition associated with the semioxidized species[37] on the basis of its band-shape and position. In confirmation of this assignment, after fixed potential electrolysis was maintained at 1.0 V for prolonged periods the IVCT band disappeared due to formation of the diradical cation. In the case of **BD2**, the process was completely reversed by applying a fixed potential of −0.1 V, but this was not so for **BD1** where partial destruction of the compound accompanied redox cycling.

For **BD3** the initial absorption spectrum is severely perturbed by strong exciton coupling (Figure 7). Oxidative electrolysis causes a marked change for the absorption spectrum and also in the degree of exciton coupling. The radical cation is less apparent in the spectrum but the onset of the IVCT band is seen at lower energy as shown in the inset to Figure 7. Finally, **BD4** behaves much like **BD3** under oxidative electrolysis (see the Supporting Information). The initial exciton coupling becomes broken, and the radical cation can

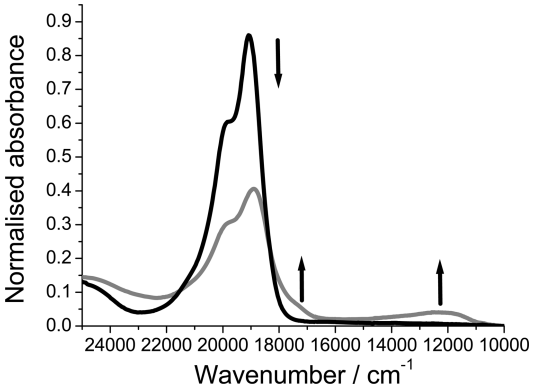

FIGURE 6. Observed changes in the absorbance profile of **BD2** upon fixed potential oxidation (1.0 V vs Fc^+/Fc ($c \approx 0.4 \times 10^{-6}$ M, DCM, 0.2 M TBATFB), using a conventional OTTLE cell: starting spectrum (black line) and final spectrum (gray line). Arrows indicate change over some 7 min.

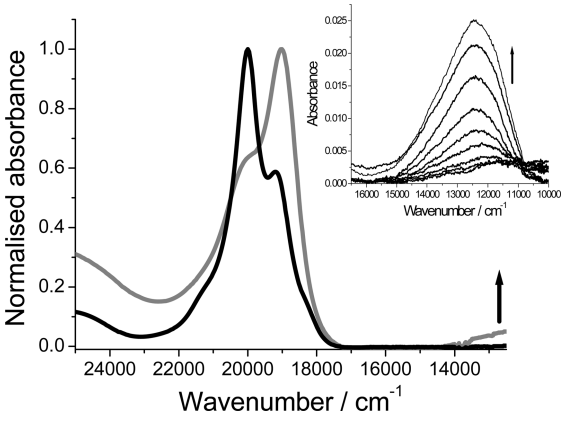

FIGURE 7. Observed changes in the absorbance profile of **BD3** upon fixed potential oxidation (1.0 V vs Fc^+/Fc ($c \approx 0.4 \times 10^{-6}$ M, DCM, 0.2 M TBATFB), using a conventional OTTLE cell: the black line indicates the starting absorption profile, while the gray line indicates the formed absorption profile after 7 min. The inset shows expansion of the grow-in of the observed intervalence charge-transfer band.

be seen on the red edge of the main absorption band while the IVCT transition is prominent at long wavelength. Again, these spectral changes could be reversed on application of a reductive potential. Although oxidation proceeds smoothly for **BD4** in tetrahydrofuran (THF) solution, there is no obvious sign of the IVCT transition under these conditions. This is presumably because THF favors a more open conformation for the mono-oxidized species where the two Bodipy rings are kept apart. Electrolysis causes loss of exciton coupling. No IVCT absorption bands could be observed on reductive scans.

$$\Delta q = \frac{\Delta E}{\sqrt{\Delta E^2 + 4{V_{12}}^2}} \quad (1)$$

$$V_{12} = \frac{0.0206\nu_{max}}{d}\sqrt{\frac{\varepsilon_{IVCT}\Delta\nu}{\nu_{max}}} \quad (2)$$

The oxidative chemistry observed for these Bodipy-based dimers can be likened to the situation found with guanine (G) residues in DNA where the oxidation potential is decreased

(36) (a) Hattori, S.; Ohkubo, K.; Urano, Y.; Sunahara, H.; Nagano, T.; Wada, Y.; Tkachenko, N. V.; Lemmetyinen, H.; Fukuzumi, S. *J. Phys. Chem. B* **2005**, *109*, 15368. (b) Duvanel, G.; Banerji, N.; Vauthey, E. *J. Phys. Chem. A* **2007**, *111*, 5361.

(37) Coropceanu, V.; Gruhn, N. E.; Barlow, S.; Lambert, C.; Durivage, J. C.; Bill, T. G.; Nöll, G.; Marder, S. R.; Brédas, J.-L. *J. Am. Chem. Soc.* **2004**, *126*, 2727.

TABLE 2. Parameters Extracted from Fitting the IVCT Transition to the Hush Model[a]

compd	d_{MM}/Å	ν_{MAX}/cm^{-1}	$\Delta\nu$/cm^{-1}	ε_{IVCT}/M^{-1} cm^{-1}	ΔE^b/cm^{-1}	V_{12}/cm^{-1}	Δq^c
BD1	6.35	11 905	1 155	4 680	565	820	0.325
BD2	5.65	12 090	1 785	4 480	805	1 130	0.335
BD3	4.56	12 240	1 905	4 800	2 095	1 505	0.575
BD4	4.90	12 170	1 770	4 900	1 695	1 360	0.530

[a]See eq 2. [b]Peak separation from cyclic voltammogram. [c]See eq 1.

upon formation of GG doublets and GGG triplets.[38] Here, charge delocalization is believed to play an important role in controlling the oxidation potential and thereby concentrating any oxidative damage at multiple guanine sites.[39] The level of charge distribution over the dimer (Δq) can be expressed in terms of eq 1, where ΔE is the difference in half-wave potential for the two Bodipy units comprising the dimer and V_{12} is the electronic coupling element.[40] These two parameters can be obtained from the cyclic voltammetric and spectroelectrochemical studies, respectively, and are collected in Table 2. In determining values for V_{12} it is necessary to analyze the IVCT band in terms of Hush theory[41] (eq 2) and the relevant parameters (namely, the wavenumber corresponding to the peak maximum (ν_{MAX}), the molar absorption coefficient at the maximum (ε_{IVCT}), and the half-width of the absorption band ($\Delta\nu$) fitted as a Gaussian component) are also collected in Table 2. For the distance (d_{MM}) between the two redox centers, we have used the closest contact between the two Bodipy rings as represented by the separation of the meso carbon atoms in the dimer. It can be seen that V_{12} is large in all cases but does show a marked sensitivity toward the molecular geometry, increasing from 820 cm^{-1} for **BD1** to 1465 cm^{-1} for **BD3**. The extent of charge distribution follows a similar pattern and increases from ca. 30% for both **BD1** and **BD2** to almost 60% for **BD3**. This last species exhibits a very high degree of charge delocalization over the two Bodipy units at the monooxidized state. Clearly, this effect is a consequence of the cofacial alignment of the two chromophores and their short separation, although the effect is far from quantitative.

Exciton Coupling. The above discussion has alluded to exciton coupling between the Bodipy units in some of the dimers described herein. Such interactions are apparent from the split absorption bands in solution and Figure 8 shows the relevant portion of the UV−visible absorption spectra recorded from cyclohexane solution at ambient temperature. Now, the control compound **BD5** shows a conventional absorption spectral profile consisting of a narrow band (fwhm = 525 cm^{-1}) centered at 526 nm with a vibronic progression stretching toward higher energy. The molar absorption coefficient (ε_{MAX}) measured at the absorption peak is 132 600 M^{-1} cm^{-1}, which is in good agreement with values measured for mononuclear Bodipy dyes (and allowing for the fact that **BD5** contains two such units). There is a weaker absorption band at higher energy (i.e., around 400 nm) that corresponds to the S_0-S_2 transition but there is no indication for self-association of the chromophores in

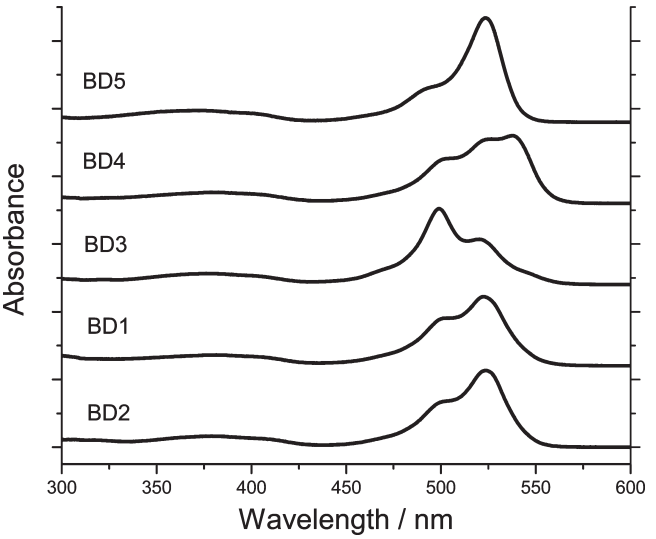

FIGURE 8. Absorption spectra of the various dimers recorded in cyclohexane at room temperature.

cyclohexane solution, even at low temperatures. The absorption maximum (λ_{MAX}) moves only slightly as the solvent polarity is changed and in accord with the results of Boens et al.,[42] which shows that λ_{MAX} is slightly sensitive to the polarizability of the surrounding medium. The reference compound displays comparable behavior.

$$\Delta\psi = \frac{|M|^2}{R^3}\left(1+\sin^2\left\{\frac{\beta}{2}\right\}\right) \qquad (3)$$

The absorption spectra recorded for **BD3** and **BD4** in cyclohexane solution are perturbed by exciton coupling, this having the effect of splitting the transitions (Figure 8). These spectra are unaffected by dilution. Exciton coupling also splits the vibronic band into two principal components. Fitting the entire S_0-S_1 absorption envelope to the sum of six Gaussian bands of common half-width (fwhm = 490 cm^{-1}) allows determination of the exciton splitting ($\Delta\psi$) as 735 and 655 cm^{-1} respectively for **BD3** and **BD4**. For both **BD1** and **BD2** (Figure 8) the lowest energy absorption transition is not split, at least at room temperature, but the band is broadened. Fitting to a series of Gaussian components as above indicates that $\Delta\psi$ is much reduced for these dimers, with values of 200 and 230 cm^{-1}, respectively, being obtained for **BD1** and **BD2** in dilute cyclohexane solution. According to the simple exciton coupling theory introduced

(38) (a) *Long-Range Charge Transfer in DNA*; Topics in Current Chemistry 236/237; Schuster, G. B., Ed.; Springer: Berlin, Germany, 2004. (b) Lewis, F. D.; Letsinger, R. L.; Wasielewski, M. R. *Acc. Chem. Res.* **2001**, *34*, 159.

(39) Senthilkumar, K.; Grozema, F. C.; Guerra, C. F.; Bickelhaupt, F. M.; Siebbels, L. D. A. *J. Am. Chem. Soc.* **2003**, *125*, 13658.

(40) Voityuk, A. A. *J. Phys. Chem. B* **2005**, *109*, 10793.

(41) Hush, N. S. *Prog. Inorg. Chem.* **1967**, *8*, 391.

(42) (a) Qin, W.; Baruah, M.; Van der Auweraer, M.; De Schryver, F. C.; Boens, N. *J. Phys. Chem. A* **2005**, *109*, 7371. (b) Baruah, M.; Qin, W.; Flors, C.; Hofkens, J.; Vallée, R. A. L.; Beljonne, D.; Van der Auweraer, M.; De Borggraeve, W. M.; Boens, N. *J. Phys. Chem. A* **2006**, *110*, 5998. (c) Qin, W.; Baruah, M.; Stefan, A.; Van der Auweraer, M.; Boens, N. *ChemPhysChem* **2005**, *7*, 2343. (d) Baruah, M.; Qin, W.; Basarić, N.; De Borggraeve, W. M.; Boens, N. *J. Org. Chem.* **2005**, *70*, 4152.

TABLE 3. Parameters Associated with Exciton Coupling for the Various Dimers in Cyclohexane Solution at Room Temperature

compd	$\Delta\psi$/cm^{-1}	R_{CC}/Å	ε_{max}[a]/M^{-1} cm^{-1}	β/deg	$\lvert M\rvert$[b]/Å
BD1	200	7.36	146 600	41.32	0.027
BD2	230	6.55	129 300	36.95	0.024
BD3	735	4.73	100 400	8.57	0.028
BD4	655	5.50	100 000	15.4	0.033

[a] ε_{max} values were recorded for the dimer in CH_2Cl_2. [b] From eq 3.

by Kasha[43] and extended by Gouterman,[44] the magnitude of $\Delta\psi$ for dimers of the type considered here is established by the "bite angle" (β) and by the mean separation distance (R_{CC}) between centers of the transition dipole moments on the two Bodipy units. Indeed, $\Delta\psi$ can be considered in terms of eq 3 where M is the transition dipole moment for the dimer absorption band. The relevant data are available from X-ray crystallography for most of the compounds but for **BD4** we have relied on molecular dynamics simulations to give a representation of the π-stacked dimer; here $\beta = 15.4°$ and $R_{CC} = 5.5$ Å. This approach allows estimation of $|M|$ for each of the dimers (Table 3). The derived values are relatively insensitive to changes in structure, corresponding to an average value of 0.028 Å, as might be expected in view of the common optical transition involved. It is, however, quite clear that the level of exciton coupling is controlled by the internuclear distance.

Concluding Remarks

By adapting a synthetic strategy developed for the isolation of porphyrin dimers, it has been possible to synthesize a series of Bodipy-based dimers that vary systematically in their molecular topology. A subtle difference between these systems and the porphyrin analogues, highlighted by **BD3**, is that fluorine−fluorine interactions prohibit perfect face-on-face overlap, a feature that prevents optimum π-orbital overlap between the neighboring Bodipy units. The Bodipy compounds are readily amenable to detailed examination by NMR spectroscopy and such studies, aided by single-crystal X-ray diffraction work, allow elucidation of the molecular structure in solution as well as in the solid state. Electronic interactions between the two Bodipy units cause perturbation of the cyclic voltammograms and the UV−visible absorption spectra. In the former case, there is a progressive fall in the half-wave potential for one-electron oxidation of the dimer with increasing levels of charge delocalization. Simultaneously, the oxidation peak is split by larger amounts due to delocalization. Under the same conditions, the S_0-S_1 absorption band is split to increasing levels due to exciton coupling and it is apparent that a linear relationship holds between ΔE and $\Delta\psi$. This situation arises because of the similar geometries that must hold for the ground state and mono-oxidized species in solution. It is interesting to note that a similar but less pronounced effect is noted for the electrochemical reduction of the dimers. The next phase of the work will involve examining if comparable levels of electronic interaction persist for the excited state and it is pertinent to note that excimer emission has been reported for a dimer similar to **BD3**.

(43) Kasha, M.; Rawls, H. R.; Ashraf El-Bayoumi, M. *Pure Appl. Chem.* **1965**, *11*, 371.
(44) Gouterman, M.; Holten, D.; Lieberman, E. *Chem. Phys.* **1977**, *25*, 139.

Experimental Section

Full details of experimental methods used and the X-ray crystallographic data can be found in the Supporting Information. All reactions were carried out under a dry nitrogen atmosphere.

Preparation of BD1. To a stirred mixture of 2,4-dimethyl-3-ethylpyrrole (0.61 mL, 4.5 mmol, 4.2 equiv) and 4,6-dibenzothiophenedicarbaldehyde (0.27 g, 1.1 mmol, 1 equiv) in DCM (200 mL) was added 2 drops of TFA. The reaction was stirred at room temperature until TLC showed complete consumption of the aldehyde. Then, DDQ (0.62 g, 2.75 mmol, 2.5 equiv) was added in a single portion and the reaction was stirred overnight at room temperature. *N*,*N*-Diisopropylethylamine (2.2 mL, 12.5 mmol, 11.4 equiv) and $BF_3\cdot Et_2O$ (2.23 mL, 17.6 mmol, 16 equiv) were added, and the reaction mixture was again stirred overnight at room temperature, then it was washed with water (3 × 100 mL) and brine (3 × 100 mL). The separated organic fractions were dried ($MgSO_4$), filtered, and evaporated under vacuum to yield a black/dark violet residue with a green tint. The residue was chromatographed on silica gel (DCM/hexane 1:3) to afford a red solid (0.20 g, 23%). Mp > 300 °C. ^{1}H NMR (d_8-THF, 400 MHz): δ (ppm) 8.27 (d, J = 7.7 Hz, 2H), 7.61 (t, J = 7.7 Hz, 2H), 7.36 (d, J = 7.7 Hz, 2H), 2.49 (s, 12H), 2.21 (q, J = 7.5 Hz, 8H), 1.08 (s, 12H), 0.90 (t, J = 7.5 Hz, 12H). ^{13}C NMR (d_8-THF, 75 MHz): δ (ppm) 154.8, 139.8, 137.6, 136.2, 136.0, 132.9, 130.9, 129.9, 127.3, 125.8, 122.1, 17.0, 14.5, 12.7, 10.7. ^{11}B NMR (d_8-THF, 160 MHz): δ (ppm) −0.153 (t, J_{av} = 34.4 Hz). ^{19}F NMR (d_8-THF, 470 MHz): δ (ppm) −145.37 (q, J_{av} = 31.78 Hz). EI-MS: m/z calcd for $C_{46}H_{50}B_2F_4N_4S$ 789, found 789. Elemental analysis calcd (found) for $C_{46}H_{50}B_2F_4N_4S$: C 70.06 (70.31), H 6.39 (6.51), N 7.10 (7.01).

Preparation of BD2. A similar procedure to that described above was followed, using 2,4-dimethyl-3-ethylpyrrole (1.14 mL, 8.4 mmol, 4.2 equiv), 4,6-dibenzofurandicarbaldehyde (0.45 g, 2 mmol, 1 equiv), DCM (200 mL), TFA (2 drops), *N*,*N*-diisopropylethylamine (3.99 mL, 22.9 mmol, 11.4 equiv), and $BF_3\cdot Et_2O$ (4.07 mL, 32.1 mmol, 16 equiv). Chromatography (silica gel) DCM/hexane (1:1). Yield 0.27 g, 18%. Mp > 300 °C. ^{1}H NMR (d_8-THF, 400 MHz): δ (ppm) 8.12 (d, J = 7.31 Hz, 2H), 7.51 (t, J = 7.3 Hz, 2H), 7.34 (d, J = 7.3 Hz, 2H), 2.51 (s, 12H), 2.21 (q, J = 7.5 Hz, 8H), 1.07 (s, 12H), 0.88 (t, J = 7.5 Hz, 12H). ^{13}C NMR (d_8-THF, 75 MHz): δ (ppm) 154.2, 153.4, 137.4, 133.5, 132.8, 131.1, 128.8, 124.5, 124.1, 121.4, 120.6, 16.9, 14.5, 12.6, 10.7. ^{11}B NMR (d_8-THF, 160 MHz): δ (ppm) −0.134 (t, J_{av} = 31.98 Hz). ^{19}F NMR (d_8-THF, 470 MHz): δ (ppm) −144.49 (m, 2F), −145.78 (m, 2F). EI-MS: m/z calcd for $C_{46}H_{50}B_2F_4N_4O$ 773, found 773. Elemental analysis calcd (found) for $C_{46}H_{50}B_2F_4N_4O$: C 71.52 (71.73), H 6.52 (6.59), N 7.25 (7.09).

Preparation of BD3. A similar procedure to that described above was followed, using 2,4-dimethyl-3-ethylpyrrole (7 mL, 52.1 mmol, 4.2 equiv), 9,9-dimethyl-9*H*-xanthene-4,5-dicarbaldehyde (3.31 g, 12.4 mmol, 1 equiv), DCM (500 mL), TFA (2 drops), DDQ (7.03 g, 31 mmol, 2.5 equiv), *N*,*N*-diisopropylethylamine (24.62 mL, 141 mmol, 11.4 equiv), and $BF_3\cdot Et_2O$ (25.14 mL, 198 mmol, 16 equiv). Chromatography (silica gel) DCM. Yield 0.5 g, 5%. Mp > 300 °C. ^{1}H NMR (d_8-THF, 400 MHz): δ (ppm) 7.65 (d, J = 7.8 Hz, 2H), 7.19 (t, J = 7.8 Hz, 2H), 7.01 (d, J = 7.8 Hz, 2H), 2.39 (s, 12H), 2.18 (m, 4H), 2.07 (m, 4H), 1.71 (s, 6H), 1.22 (s, 12H), 0.86 (t, J = 7.5 Hz, 12H). ^{13}C NMR (d_8-THF, 75 MHz): δ (ppm) 154.4, 147.6, 145.3, 136.8, 135.5, 132.5, 131.5, 130.8, 129.6, 128.2, 124.9, 120.9, 35.2, 33.6, 17.7, 14.9, 12.7, 10.8. ^{11}B NMR (d_8-THF, 160 MHz): δ (ppm) −0.59 (t, J_{av} = 33.21 Hz). ^{19}F NMR (d_8-THF, 470 MHz): δ (ppm) −145.08 (m, 2F), −146.96 (m, 2F). EI-MS: m/z calcd for $C_{49}H_{56}B_2F_4N_4O$ 814, found 814. Elemental analysis calcd (found) for $C_{49}H_{56}B_2F_4N_4O$: C 72.25 (72.19), H 6.93 (6.89), N 6.88 (6.94).

Preparation of BD4. A similar procedure to that described above was followed, using 2,4-dimethyl-3-ethylpyrrole (2.38 mL, 17.6 mmol, 4.2 equiv), bis(2-formylphenyl) ether (0.95 g, 4.2 mmol, 1 equiv), DCM (200 mL), TFA (2 drops), DDQ (2.38 g, 10.5 mmol, 2.5 equiv), *N*,*N*-diisopropylethylamine (8.3 mL, 47.8 mmol, 11.4 equiv), and $BF_3.Et_2O$ (8.51 mL, 67 mmol, 16 equiv). Chromatography (silica gel) toluene. Yield 0.52 g, 16%. Mp > 300 °C. ^{1}H NMR (d_8-THF, 400 MHz): δ (ppm) 7.44 (td, J = 8.3 Hz, J' = 1.8 Hz, 2H), 7.27 (dd, J = 8.3 Hz, 1.8 Hz, 2H), 7.22 (d, J = 8.1 Hz, 2H), 7.16 (d, J = 8.1 Hz, 2H), 2.42 (s, 12H), 2.32 (m, 8H), 1.31 (s, 12H), 0.91 (t, J = 7.5 Hz, 12H). ^{13}C NMR (d_8-THF, 75 MHz): δ (ppm) 153.4, 153.1, 136.9, 135.3, 132.3, 131.2, 130.8, 130.0, 127.5, 123.9, 116.9, 16.8, 13.9, 11.6, 10.3. ^{11}B NMR (d_8-THF, 160 MHz): δ (ppm) −0.47 (t, J_{av} = 33.22 Hz). ^{19}F NMR (d_8-THF, 470 MHz): δ (ppm) −145.92 (q, J_{av} = 32.49 Hz). EI-MS: m/z calcd for $C_{46}H_{52}B_2F_4N_4O$ 774, found 774. Elemental analysis calcd (found) for $C_{46}H_{52}B_2F_4N_4O$: C 71.33 (71.35), H 6.77 (6.71), N 7.23 (7.19).

Preparation of BD5. A similar procedure to that described above was followed, using 2,4-dimethyl-3-ethylpyrrole (2.83 mL, 21 mmol, 4.2 equiv), 4-(4-formylphenoxy)benzaldehyde (1.13, 5 mmol, 1 equiv), DCM (200 mL), TFA (2 drops), DDQ (2.83 g, 12.3 mmol, 2.5 equiv), *N*,*N*-diisopropylethylamine (9.9 mL, 56.9 mmol, 11.4 equiv), and $BF_3 \cdot Et_2O$ (10.12 mL, 79.8 mmol, 16 equiv). Chromatography (silica gel) DCM/hexane (2:5). Yield 1.01 g, 26%. Mp 292−295 °C. ^{1}H NMR ($CDCl_3$, 400 MHz): δ (ppm) 7.27 (d, J = 7.8 Hz, 4H), 7.15 (d, J = 7.8 Hz, 4H), 2.52 (s, 12H), 2.30 (q, J = 7.5 Hz, 8H), 1.39 (s, 12H), 0.97 (t, J = 7.5 Hz, 12H). ^{13}C NMR ($CDCl_3$, 75 MHz): δ (ppm) 157.2, 153.9, 139.3, 132.9, 131.1, 130.9, 129.0, 128.2, 119.4, 17.1, 14.6, 12.5, 11.9. ^{11}B NMR ($CDCl_3$, 160 MHz): δ (ppm) −0.1343 (t, J_{av} = 33.22 Hz). ^{19}F NMR ($CDCl_3$, 470 MHz): δ (ppm) −145.65 (q, J_{av} = 30.33 Hz. EI-MS: m/z calcd for $C_{46}H_{52}B_2F_4N_4O$ 774, found 774. Elemental analysis calcd (found) for $C_{46}H_{52}B_2F_4N_4O$: C 71.33 (71.29), H 6.77 (6.78), N 7.23 (7.15).

Acknowledgment. We thank the Engineering and Physical Sciences Research Council (EPSRC) and Newcastle University for financial support, and the EPSRC-supported Mass Spectrometry Service at Swansea for obtaining the mass spectra. Prof. William McFarlane is thanked for expert help with the NMR studies, and Drs. Gary Nichol and Simon Teat are thanked for collected synchrotron diffraction data at the Advanced Light Source, Berkeley, for **BD1** and **BD3**.

Supporting Information Available: Experimental details, X-ray structure data, and assorted additional spectra, structures, and NMR data. This material is available free of charge via the Internet at http://pubs.acs.org.